A Brief Comparison: Ion-Trap and Silicon-Based Implementations of Quantum Computation

Tzvetan Metodiev[†], Dean Copsey[†], Frederic T. Chong[†],
Isaac Chuang[◇], Mark Oskin[‡],and John Kubiatowicz[◦]
[†] University of California at Davis, [◇] Massachusetts Institute of Technology,
[‡] University of Washington, [◦] University of California, Berkeley

ABSTRACT

Recent progress in the physical implementation of quantum computers has taken quantum computing away from science fiction and placed it on a very real time table. Prior work [5, 21] has examined some of the basic constraints of building scalable quantum computers using silicon-based technologies. This research has focused on the Kane [11] model of phosphorus atoms embedded in silicon. In this paper, we extend this work by examining another promising quantum technology: ion-traps [12].

Ion traps, although perhaps not as scalable as proposed silicon approaches, are closer to reality and offer some experimentally verified data with which to test architectural designs. Furthermore, ion traps offer the ability to exploit physical symmetries, which reduce sensitivity to environmental noise via small *decoherence-free subspaces*. Finally, ion traps have demonstrated the physical motion of a quantum bit, offering a medium-distance communication mechanism.

1. INTRODUCTION

The development of fault-tolerant quantum error correction [9, 22, 24] provided a clear way to tackle the main obstacle of building large-scale quantum computers - *decoherence*, which is the alteration of the quantum state of a qubit due to contact with its environment. Fault-tolerant error correction allows for the construction of a reliable quantum computer from an unreliable device technology as long as each elementary component of the architecture has a probability of failure below an estimated threshold value of approximately 10^{-4}. This value drops significantly if the following two assumptions are **not** met: 1) errors in the quantum circuits are independent; 2) the circuits themselves must exhibit maximum parallelism.

The above requirements for fault-tolerant quantum computation are dependent to a significant extent on the physical layout of the system. In this paper, we analyze the constraints that must be satisfied in the architectural design of a quantum computer using ion-trap technology. We also provide a brief comparison of the ion-trap model [2] with the silicon based model of Skinner, *et. al.*, [10].

The ion-trap scheme to quantum information processing is the only approach known thus far to experimentally satisfy all of the DiVincenzo criteria [6], which establish some basic requirements for constructing a reliable quantum computer. These criteria include: state preparation, quantum logic gates and measurement of states [2]. The proposed device technology analyzed in our previous work [5, 21] is also thought to satisfy DiVincenzo's criteria, but it has not yet been experimentally demonstrated. What is appealing about both of these proposals is the fact that they can be implemented with silicon technologies, a much accepted and studied technology.

Ion traps are also the only known approach that allows for the generation and manipulation of the entangled states of 2 to N qubits deterministically [12]. One ion-trap scheme using *quantum charge coupled devices*, proposed by Kielpinski, is suited for our analysis since its implementation is readily made possible by the standard lithographic methods developed for silicon micromachining [12]. It consists of a large number of interconnected ion traps, each with a number of ions held together by an RF quadrupole field. The qubits are held in pairs of hyperfine energy sublevels of the ions. Information transfer is carried out by changing the operation voltages of the traps and thus moving ions between them; a schematic is shown in Figure 2. This type of information sharing lets us explore how *ballistic transport* can be used for transporting states of qubits as a less restrictive communication channel than swapping.

In the next section we describe the Kane phosphorus-in-silicon [11] and Kielpinski [2] ion-trap technologies. We follow this with a discussion of fault tolerant computation within these technologies (Section 3), and a reliability analysis in Section 4. Conclusions and future work are described in Section 5.

2. TECHNOLOGY MODELS

In this section, we describe the main characteristics of the Kane [11] phosphorus-in-silicon and Kielphinski [2] ion trap device technologies.

2.1 Silicon Based Kane Model

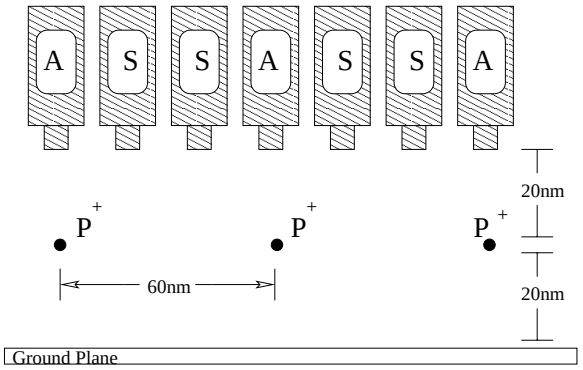

Figure 1: The Kane Model: the phosphorus is the donor whose nucleus has opposite spin with the electron enabling the storage of quantum states. The figure shows two embedded qubits in silicon.

The Skinner-Kane model [10, 25] analyzed in much greater detail elsewhere [11, 21, 5] is briefly summarized here. The basic idea is outlined in Figure 1, where qubits are laid out in silicon. The quantum states are stored in electron-donor spin pairs ($e^- - {}^{31}P^+$).

Single qubit operators are implemented via rotations around the $\hat{z}$-axis through pulses on the classical A gates positioned above the phosphorus atoms. The $\hat{x}$-axis rotations are achieved with a globally applied magnetic field. The other classical gates in the picture (S-gates) are used for two-qubit interactions, where an electron is moved from one phosphorus nucleus to the next. The distance between the atoms is under debate and is believed to be between 15 and 100 nanometers. The value of 60nm was assumed in our previous work to balance spatial constraints and error tolerances.

2.2 Ion Trap Model

The ion-trap model proposed and experimented on by Kielpinski, *et. al.*, [2, 12, 16], has been built on the initial proposal by Cirac and Zoller [4] with the following key features:

1 States of qubits are defined by the hyperfine interactions between the nuclear and electronic states of each ion, which are laid out in a linear RF trap.
2 Universal quantum gates are implemented by using laser beams to "excite the collective quantized motion of the ions [4]."
3 Quantum information exchange is done via Coulombic interactions between the ions.
4 Multy-qubit systems are implemented by appending ions on the trap.

The Kielpinski model [2] possesses all of the above, but proposes a large scale quantum charge-coupled device (QCCD) of interconnected ion traps, where quantum information is stored in memory regions and moved to special interaction regions for manipulation. This not only eliminates the need for lengthy arrays, but, as shown in Figure 2, is also a highly scalable model. One of the most important features of this model is that it has

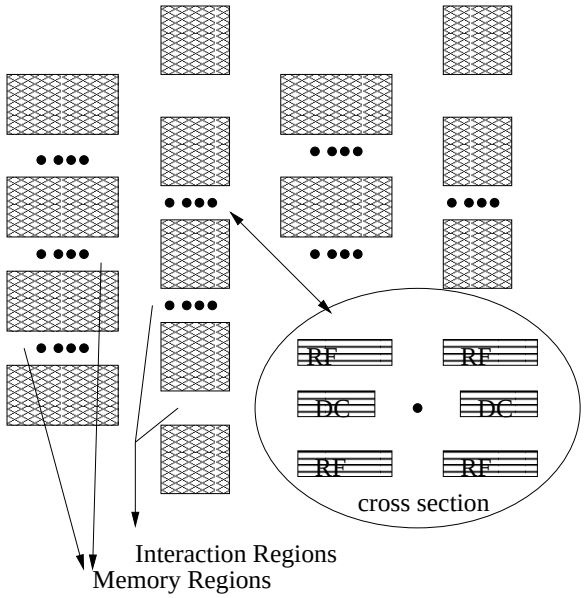

Figure 2: Schematic of interconnected ion traps. The zoomed section is a cross view of the trap axis, where the top and bottom electrodes are the r.f. electrodes enclosing the d.c. ones in the middle.

been built with current micro-machining techniques in alumina, and that ballistic transportation of an ion from one trap to another has been demonstrated [16].

The design [12] in Figure 2 is boron-doped <100>-cut Si wafers stacked together in three layers, with the middle layer carrying a DC voltage used for axial confinement of the ions, and outer layers contain an RF voltage needed for the radial confinement. The ions experimented with are Be^+, with the qubit state composed of the two hyperfine levels. Raman transitions [16, 18] provide the coupling between $|\downarrow\rangle$ and $|\uparrow\rangle$ to put the qubit into a superposition. Single qubit operators are achieved by applying laser beams to each ion [4]. Universal quantum gates can be implemented by exiting the "collective quantized motion" of the ions.

The Molmer-Sorensen gate implemented in the form of laser pulses [17, 18] produces an N-qubit entangled state. Experimentally, this was done in [18] with 2 and 4 ions with efficiency of ~ 0.8, where each time ions were cooled to their quantum ground state (eg. $|\downarrow\rangle$). Doppler and Raman cooling [16, 18] were used to pump each ion to the ground $|\downarrow\rangle$ state. Measurement was performed by applying circularly polarized light and counting the number of photons scattered. Measurement accuracy near 100% and a timescale of about 200μs were observed during detection.

2.3 Analysis and Comparison

In this section we explore some of the key architectural differences that arise from these two device technologies. Notably these include differences in communication primatives, error correction support, and scalability.

2.3.1 Transport - Static versus Dynamic

In contrast with the Skinner-Kane model, the ions in the traps are not confined to a single position. While usually trapped, but they can be shuffled around by changing the potentials of the trapping electrodes. In the Kane model information is passed via neighbor-to-neighbor SWAPs. In comparison, by moving the ions the idea of *ballistic transport* can be exploited. Experiments on ion transport have been done in [16] on a trap made with alumina wafers instead of silicon. An ion was transported 10^6 times between two trapping electrodes over a total distance of 1.2mm at a time of $\sim 50\mu s$ without shortening the coherence time of the state.

In the Kane model the neighbor-to-neighbor *swap*s account for about 80% of the operations a qubit undergoes. SWAP operations are applied between alternating phosphorus atoms. This way the states are propagated by being swapped from atom to atom. In [21] we estimated qubit separation of 60nm with a SWAP speed of $0.57\mu s$ as estimated by Kane. Thus a distance of 1.2mm can be trasversed in $0.68s$.

Both technologies allow a different kind of transport that is irrelevant of distance and can only be applied to quantum computing: *Teleportation*. We reserve teleportation a subsection of its own later in the paper.

2.3.2 Decoherence and DFS encoding

For the success of any quantum computer, a reliable memory is essential. Interaction of a quantum system with its environment destroys the state of the system, a process we mentioned earlier as decoherence. In [13], Kielpinski, et. al. showed that collective dephasing (i.e. each qubit is coupled to the environment) is the defining limit of reliable quantum memory using ions as physical qubits. Collective dephasing is caused by the variations of the magnetic field in space. If the state of each qubit is spanned by $|\downarrow\rangle$ and $|\uparrow\rangle$, during transport the $|\uparrow\rangle$ state acquires a relative phase α as $e^{i\alpha}|\uparrow\rangle$. Since the down state does not change, the phase cannot be factored out.

Researchers [8, 13, 15] have exploited the symmetry behind the fact that if a logical qubit is encoded in a way such that its state is spanned by $|0\rangle = |\downarrow\uparrow\rangle$ and $|1\rangle = |\uparrow\downarrow\rangle$ using two physical qubits (i.e. two ions), then the dephasing of the up states of both ions can be canceled. Thus it becomes irrelevant to the extent that the probability of measuring each one of the two states does not change.

This type of decoherence-free subspace (DFS) encoding creates an attractive low-level for of error correction. As long as the magnetic field strength is the same for each qubit, the DFS offers a very reliable protection against collective dephasing. Later in this paper we describe results that use a DFS in the analysis of fault tolerant error correcting algorithms.

It is speculated that type of small DFS may also work in the Skinner-Kane technology model, but no experimental work has yet progressed towards this.

2.3.3 Scalability and Architectural Constraints

Since ions are shuffled around via ballistic transport and DFS encoding, which ensures minimum motional decoherence, the trapping electrodes need not be much larger than the trapped ions themselves, which could provide for a scalable environment. The interconnected ion traps allow for a high degree of parallelism. Due to the Coulomb forces on each ion, the ions themselves are also isolated from one other allowing simultaneous read out, and operations can be applied on different memory regions at the same time. One thing to keep in mind is that for the ions to be isolated from one another they need to be at least $10\mu m$ apart.

The main architectural constraint with ion traps is outlined in [7, 14, 16, 18]. One problem is that ions aquire motional heating when shuttled around. This heating can be overcome by having small number of ions in the arrays and adding an extra ion for each ion already there. The extra ions are kept at constant ground state and the rest of the ions can be sympathetically cooled through those extra ions. As the number of ions grows, adding extra qubits to the arrays adds extra degrees of freedom to the fluctuations. Thus an array of interconnected distinct ion traps is proposed: Figure 2. The limit of qubits in each array is given to be two–to–five, thus we will assume four. The reader should keep in mind that all qubits consist of two physical qubits encoded as one logical DFS qubit, so the traps will only have two "logical qubits." Logical gates on the ions are applied with laser pulses, which poses yet another limit to scalability concern.

The Kane proposal operates on a much smaller scale with 60nm qubit separation, but this number poses a problem for the requirement of efficient classical control. The Kane model operates at a temperature of less than one degree kelvin; thus classical control gates (A gate and S gates) will suffer quantum effects and must be at least 100nm in dimension each. The process of actually embedding the phosphorus atoms in silicon has not been achieved yet and is very difficult. The leading work has been done in [11]. The classical control gates must be about 10nm at the tip. Research is promising to make this scale possible [3, 23].

Scalability constraints are best described with the analysis of the most important quantum operation: fault tolerant error correction. Fault tolerant quantum computation can be implemented by recursively applying error correction and encoding the ions in DFS. Due to the ballistic transport idea qubits need not be in close proximity for error correction. Section 3 sets up a network for fault tolerant error correction using trapped ions.

2.3.4 Teleportation

Teleportation starts with two qubits entangled to form

an EPR pair, keeping one qubit at the source location and sending the other to the destination. To transport a qubit $|a\rangle$, it is interacted with the source qubit, measured, and then the classical results of this measured are sent to the destination. Using this classical information the state is recreated in the other half of the EPR pair previously communicated.

For both device technology proposals the separation distance between the two qubits from the EPR pair can be discounted when computing the latency of the teleportation operation. The bandwidth of a teleportation channel, however, is proportional to the reliability of the underlying technology [21].

3. FAULT-TOLERANT COMPUTATION

We turn now to an outline of the basic constructions of fault-tolerant quantum computation. This is a rather involved subject (for which the reader is referred to the literature [19]), but three essential ideas are covered in this brief introduction: 1) what quantum error correction is; 2) using fault tolerant procedures; 3) provide a brief explanation of recursive error correction [1].

The main result we build upon [1] can be stated as follows: *A quantum circuit containing N error-free gates can be simulated with a probability of failure of at most* ε *using* $O(\text{poly}(\log(N/\varepsilon))N)$ *imperfect gates which fail with probability p as long as* $p < p_{th}$*, where* p_{th} *is a constant threshold that is independent of* N.

3.1 Quantum Error Correction

Peter Shor [24] performed the ground–breaking work on quantum error correction. What follows is a brief summary of his work, as well as that of Steane [26].

In order to implement quantum error correction one needs to modify traditional error correcting codes, since qubits no longer suffer just a bit flip error as in classical computation. Due to the more complex representation of each qubit state (eg. superposition), qubits now suffer not only amplitude and phase flip errors, but almost any single-qubit unitary operator error becomes possible.

Moreover, quantum computation is challenged by a fundamental result of quantum mechanics – the no-cloning theorem – which prevents us from copying an arbitrary known quantum state [29]. This means that quantum computation cannot use the classical methods of error correction, but that it must adopt a new set of error correcting codes.

The overall principle of quantum error correction is very similar to classical computation where a majority vote is taken to detect the type of error that has occurred. The difference is that physical qubits are encoded into logical qubits using the properties of entanglement. Once the encoding is done, parity is measured using the two qubit CNOT operator instead of the classical XOR gate. Entanglement is used to avoid direct measurement of the state of the system and to provide fault tolerance from one step to the next.

A remarkable result that made quantum error correction possible is the fact that the spectrum of all possible continuous errors can be converted to a discrete reversible set of operators [9, 20].

In the subsection below we concentrate on two methods of encoding physical qubits: Lowest level (DFS) encoding and a second level of encoding known as the Steane [26] $[[\mathbf{7},\mathbf{1},\mathbf{3}]]$ code. Both encodings satisfy a necessary condition of fault tolerance – support of universal fault tolerant quantum logic [1].

3.2 Lowest Level Error Correction

In the Skinner-Kane proposal the lowest level encoding of qubits is the Steane $[[\mathbf{7},\mathbf{1},\mathbf{3}]]$ code. In the ion-trap model, however, the $[[\mathbf{7},\mathbf{1},\mathbf{3}]]$ code is used at the second level. This is due to the introduction of DFS encoding and the proof that universal quantum computation can be done on DFS encoded qubits [14]. DFS encoding consists of the following steps:

1 Laser cooling is used to initalize the two ions to the $|\downarrow\downarrow\rangle$ state.
2 The Sorensen-Molmer entangling gate [17] is then applied three times to the new state to realize its inverse and to produce the state consisting of the superposition of $(|\downarrow\downarrow\rangle - i|\uparrow\uparrow\rangle)$ and $(|\downarrow\uparrow\rangle - i|\uparrow\downarrow\rangle)$
3 Changing the phase difference of the two laser beams then enables the formation of the DFS encoded logical qubit.

Once the two qubits are DFS encoded into one logical qubit any quantum computation can be performed on them without the problem of a fluctuating magnetic field. The Sorensen-Molmer gate and a sequence of single qubit rotations can be combined to generate any single qubit gate on a DFS encoded qubits [13, 14]. Since all errors on qubit states are unitary evolutions, the strong and fast pulses implement the *parity-kick sequence*, which generates a gate that conjugates the error operator [14]. Conjugation is important since if U is the error operator, then we can apply the generated gate to form the dagger of U, thus when U acts again the result is the identity operator. This cancels out the error U.

3.3 Second Level Error Correction

In this subsection, we present a fault tolerant error correction network for the second level of encoding, which is readily implemented with ion-traps. We will quantify the requirements needed for an ion-trap model. A similar network for the Skinner-Kane model was presented in [5], with the results reiterated here for comparison purposes.

The network is a reproduction of Steane's 'ancilla factory' error correction method to extract the error syndrome [27]. The method consists of generating the encoded zero state $|0_L\rangle$ within an eight-qubit ancillary block, where one qubit is used to verify the generated

state. Upon successful verification within the ancillary block the $|0_L\rangle$ state is rotated by the Hadamard transformation applied bitwise to form the state $|0_L\rangle + |1_L\rangle$. In fact, two ancillary blocks are needed, with one block used for correcting bit errors and one block for correcting sign errors in the encoded qubits[1] errors. Starting with eight $|0\rangle$ ancillae the network consists of three parts:

1 Generate the $|0_L\rangle$ state using three Hadamard gates and nine CNOT operations acting as XORs.
2 Verify the encoded zero state. If at any point during the verification a bit error is encountered, the network is restarted. A sign error is not detected. However, a sign error in this case will be converted to a bit error during Step 3 causing the entire syndrome to be incorrect.
3 The third and final part is generating the encoded $|0_L\rangle + |1_L\rangle$ by applying bitwise 7 Hadamard gates to the block.

This algorithm appears to not be fault tolerant because bit errors may propagate among the qubits before the verification step and sign errors propagate among the qubits during the verification step. Both of these are acceptable, since a sign error causes an invalid syndrome and a bit error causes the network to be restarted. On the other hand Steane's design does not allow any bit errors formed during the verification to propagate among qubits. Thus the errors are uncorrelated when transferred to the block we are correcting.

The two ancillary blocks for bit and sign errors are formed and computed parallel to each other. They interact with the block to be corrected by seven XOR (eg. CNOT) gates. The subsequent measurement of the ancilla qubits extracts the resulting syndrome. The syndrome determines which, if any, qubit has an error; an X, Z, or Y operator can be applied to correct the error.

Steane finds the probability α of getting the incorrect syndrome to be ~ 0.001 for the ion-trap system he proposes [27, 28]. Since an error can be generated in the code during each syndrome measurement, he asserts that on the average the first two syndromes will be consistent with identifying the error to be corrected. The probability of two consistent syndromes is $\sim (1-\alpha)^2$.

For the Steane $[\![7,1,3]\!]$ code, each syndrome requires sixteen ancillae: eight for the block identifying bit errors, and eight for the block identifying the sign errors. Since there are two syndromes on the average for each error correction, a total of 32 ancillae are required.

Each of the two syndrome measurements requires:

- Three Hadamard and nine CNOTs to create the encoded zero state $|0_L\rangle$ in each ancillary block;
- Four qubit measurements and fifteen CNOT's to verify the $|0_L\rangle$ in each ancillary block;
- Seven Hadamard operations for the rotation of each $|0_L\rangle$ (total of fourteen);
- Additional seven Hadamard gates for the base conjugation and seven Hadamard gates before the measurement of the ancillae in the bit-error-detection ancillary block;
- Fourteen CNOTs for the communication between the two ancillary blocks and the data-qubits block;
- Fourteen measurements of the ancillae to determine the errors to be corrected.

If the time required to apply a single-qubit operator is S, a CNOT is C, and a measurement is M, then considering that the two syndromes are done sequentially, the minimum time required to correct the error is $(2S+24C+4M)+(4C+2S+2M)$.

4. ALGORITHM ANALYSIS

Although DFS encoding of qubits greatly reduces the decoherence effects, in a fault tolerant quantum computer error correction remains the most important operation. In this section we analyze the error correction algorithm presented in Section 3.1.

Naturally if a two-qubit operator is applied to two qubits, one must be brought next to the other one. This is true for both the Skinner-Kane model and the ion-trap model. The difference is in the transport.

For the Skinner-Kane model the physical atoms are not transported anywhere; their quantum states are transported via the SWAP operator. This is not a problem, since the SWAP operator is a built-in function of the technology. Generally a SWAP operator is implemented via three CNOT gates, but in this case it is only slightly more expensive than a single qubit operation. For the $[\![\mathbf{7},\mathbf{1},\mathbf{3}]\!]$ code it was determined that the time required for an error correction is a combination of the sum of the times to create the cat state, to verify it, to entangle it with the parity qubits, to uncreate it, and to measure fault tolerantly. This is multiplied by 12 because there are six parity measurements and they are performed at least twice to reduce the error probability. A third measurement would be needed if the first two disagree. And this is just the lowest level of encoding; as the encoding levels increase, each qubit is encoded to a logical qubit which itself is encoded to a logical qubit, generating exponential error improvement at the cost of exponential overhead.

With the error correction network in [5] the cost for the Skinner-Kane model was estimated to be

$$t_{ecc} \leq 336 t_{swap} + 168 t_{cnot} + t_{meas},$$

where t_{ecc} is the time for error correction, t_{swap} the time for a SWAP, t_{cnot} is the cost of a CNOT gate, and t_{meas} stands for measurement. Recalling from Skinner, Davenport, and Kane [25] that t_{cnot} is ≈ 3.2 μs, t_{swap} is ≈ 570 ns, t_{meas} is 100-200 ns, and t_{single} is ≈ 100 ns; t_{ecc} is under 362 μs.

For ion-traps, on the other hand, the lowest level of error correction uses DFS encoding with only a factor of

[1]The discussion for correcting sign errors is equivalent, except for the difference that the computations within the corresponding ancillary block are in the conjugate basis.

Operator.	Silicon	Ion-Trap
SWAP	0.57μs	6μs
Transport	$0.15m/s$	$10m/s$
Entang.	4μs	1μs
CNOT	3.2μs	2μs
Rotation	$\leq 0.3\mu$s	$\leq 24\mu$s
Hadamard	0.1μs	1.5μs

Table 1: Operations summary for the two technologies.

two overhead. Parity measurements on different qubits encoded by DFS need not be the standard parity described above. Error correction on DFS encoded qubits can be done with the application of strong and weak pulses of the SM[2] two qubit entangling gate [17], which can be made as little time as 1μs [14].

Ion trap second level encoding is the $[\![\mathbf{7},\mathbf{1},\mathbf{3}]\!]$ code described in Section 3.3, which is analogous to the Skinner-Kane lowest level encoding. This network is different than the network selected for the Skinner-Kane model, since it is simpler and Steane directed it for ion-traps. The cost of a parity measurement is greatly dependent on the physical system used, since there have been many different sizes of electrodes proposed as well as not yet demonstrated improvements.

For our analysis we make a number of assumptions based on prior work [13, 14, 16, 18]: 1) An arbitrary qubit rotation on an encoded logical qubit with DFS will take at most 24 laser pulses directly related to the SM gate for entangling two qubit states, which is roughly 1μs; 2) detection period for the state of a qubit is about 200μs; 3) a CNOT gate on two DFS encoded qubits is implemented via the four-qubit entangling SM gate for approximately 2μs; 4) A SWAP operator is equal to three CNOT gates; 5) the Hadamard gate, being the most used single qubit operator in error correction, is about 1.5μs.

In this particular error correcting network the cost depends on the time required for creating the encoded $|0_L\rangle$ state (t_{0_L}), verifying it (t_{lv}), entangling the ancilla with the data qubits together with measurement, and on the ballistic transport of the qubits (t_{tr}). The total cost is

$$t_{ecc} \leq 120t_{tr} + 76t_{cnot} + 20t_{meas},$$

which takes into account that each syndrome is done twice and assumes t_{tr} to be the time for one unit of distance, which we can assume to be about 30μm. The amount of distance travelled by the qubits depends greatly on the arrangement of the system and the material make-up of the system. Table 1 summarizes the speed of each individual operation for the two models. Using the ion-trap portion of the table and the equation above, it can be concluded that the total time for second level error correction is approximately 4314μs. However, this is the second level of encoding, a big improvement compared to the Skinner-Kane second level, which is proportional to the square of the time for the first level of encoding.

In higher levels of error correction the cost relationships will be recursive to the previous levels. The difference is that the qubits will need to travel a further distance. In [5], it was determined that the Skinner-Kane model will need to implement teleportation as its means of transportation after the fifth level of encoding. Teleportation is much cheaper than SWAPs over large distances. Teleportation is also possible for trapped ions since having a DFS encoded logical qubit and entangling it with another DFS encoded qubit produces a very reliable EPR pair.

5. CONCLUSION

Exploring the number of operations and the time constraints needed for single level and multiple level error correction, we can quantify the number of ions as well as the spatial requirements needed for the proposed ion-trap architecture. This will allow us to give a proposed layout of a large-scale quantum-memory region and processor, taking into account the mobility of the qubits and the constraints brought by this mobility.Through the detailed analysis of the lowest levels of error correction for the two models, it can be seen that for higher levels both ballistic transport and neighbor-to-neighbor interactions must be replaced by the faster method of teleportation; otherwise the speed per operation rises significantly. The recursion, although it provides us with exponential reduction of error, comes with the cost of exponential overhead for both models.

An alternative to recursive error correction is proposed by researches for the ion-trap model [14], where qubits are encoded no further than the lowest level DFS encoding. This method has not been tested experimentally, but is possible with the small interconnected arrays the model is based on. State errors are corrected always with the parrity-kick sequence from Section 2.3.2. Ion traps allow yet another method to eliminate recursion, which is the introduction of an N-ion DFS encoding. However, there is no substantial work in that direction.

In previously examined static qubit technologies as the Skinner-Kane model, the dominant factor of system reliability was the SWAP operation, since information is swapped between neighboring qubits. In the ion-trap case one can take advantage of the mobility of the qubits to transfer information and quantify more efficient recursive error correcting codes, with a focus on the spatial and temporal constraints of the technology used.

6. ACKNOWLEDGMENTS

Thanks to Daniel Lidar for the discussion on decoherence-free subspaces and ion traps. This work is supported in part by the DARPA Quantum Information, Science and

[2]for readability purposes SM will be the abreviation for the Sorensen-Molmer technique of entanglement

Technology Program, by NSF CAREER grants to Mark Oskin and Fred Chong, an NSF NER grant and a UC Davis Chancellor's Fellowship to Fred Chong.

7. REFERENCES

[1] D. Aharonov and M. Ben-Or. Fault tolerant computation with constant error. In *Proceedings of the Twenty-Ninth Annual ACM Symposium on the Theory of Computing*, pages 176–188, 1997.

[2] D. K. amd C. Monroe and D. Wineland. Architecture for a large-scale ion-trap quantum computer. *Nature*, 417:709–711, 2002.

[3] E. Anderson, V.Boegli, M. Schattenburg, D. Kern, and H. Smith. Metrology of electron beam lithography systems using holographically produced reference samples. *J. Vac. Sci. Technol.*, B-9, 1991.

[4] J. I. Cirac and P. Zoller. Quantum computations with cold trapped ions. *Phys. Rev. Lett.*, 74:4091–4094, 1995.

[5] D. Copsey, M. Oskin, T. Metodiev, F. T. Chong, I. Chuang, and J. Kubiatowicz. The effect of communication costs in solid-state quantum computing architectures. In *Proc. Symposium on Parallelism in Algorithms and Architectures (SPAA 2003)*, New York, 2003. ACM Press.

[6] D. P. DiVincenzo. The physical implementation of quantum computation. *quant-ph/0002077*, 2000.

[7] e. a. D.Kielpinski. Recent results in trapped-ion quantum computing and nist. *quant-ph/0102086*, 2001.

[8] L. Duan and G. Guo. Reducing decoherence in quantum-computer memory with all quantum bits coupling to the same environment. *Phys. Rev. A*, 57:737–741, 1998.

[9] D. Gottesman. Theory of fault-tolerant quantum computation. *Phys. Rev. A*, 57(1):127–137, 1998. arXive e-print quant-ph/9702029.

[10] B. Kane. A silicon-based nuclear spin quantum computer. *Nature*, 393:133–137, 1998.

[11] B. E. Kane, N. S. McAlpine, A. S. Dzurak, R. G. Clark, G. J. Milburn, H. B. Sun, and H. Wiseman. Single spin measurement using single electron transistors to probe two electron systems. *arXive e-print cond-mat/9903371*, 1999. Submitted to Phys. Rev. B.

[12] D. Kielpinski. Entanglement and decoherence in a trapped-ion quantum register. *Thesis, Univ. Colorado*, 2001.

[13] D. Kielpinski, V. Meyer, M. Rowe, W. I. C.A. Sacket, C. Monroe, and D. Wineland. A decoherence-free quantum memory using trapped ions. *Science*, 291:1013–1015, 1998.

[14] D. Lidar and L.-A. Wu. Encoded recoupling and decoupling: An alternative to quantum error correcting codes, applied to trapped ion quantum computation. *quant-ph/0211088*, 2002.

[15] D. A. Lidar, I. L. Chuang, and K. B. Whaley. Decoherence-free subspaces for quantum computation. *Phys. Rev. Lett.*, 81(12):2594–2597, 1998.

[16] e. a. M.A. Rowe. Transport of quantum states and separation of ions in a dual rf ion trap. *quant-ph/0205094*, 2002.

[17] K. Molmer and A. Sorensen. Multiparticle entanglement of hot trapped ions. *Phys. Rev. Lett.*, 82:1835, 1999.

[18] C. Monroe, C. Sackett, D. Kielpinski, C. L. B.E. King, V. Meyer, C. Myatt, Q. T. M. Rowe, W. Itano, and D. Wineland. Scalable entanglement of trapped ions. *AIP Conf.*, 551:173–186, 2001.

[19] M. Nielsen and I. Chuang. *Quantum computation and quantum information*. Cambridge University Press, Cambridge, England, 2000.

[20] M. A. Nielsen and I. L. Chuang. *Quantum Computation and Quantum Information*. Cambridge University Press, Cambridge, UK, 2000.

[21] M. Oskin, F. Chong, I. Chuang, and J. Kubiatowicz. Building quantum wires: The long and the short of it. In *Proc. International Symposium on Computer Architecture (ISCA 2003)*, New York, 2003. ACM Press.

[22] J. Preskill. Reliable quantum computers. *Proc. R. Soc. London A*, 454(1969):385–410, 1998.

[23] M. Sanie, M. Cote, P. Hurat, and V. Malhotra. Practical application of full-feature alternating phase-shifting technology for a phase-aware standard-cell design flow. 2001.

[24] P. Shor. Fault-tolerant quantum computation. In *37th FOCS*, 1994.

[25] A. Skinner et al. Hydrogenic spin quantum computing in silicon: a digital approach. *quant-ph/0206159*, 2002.

[26] A. Steane. Error correcting codes in quantum theory. *Phys. Rev. Lett.*, 77, 1996.

[27] A. Steane. Space, time, parallelism and noise requirements for reliable quantum computing. *quant-ph/9708021*, 1997.

[28] A. Steane and D. Lucas. Quantum computing with trapped ions, atoms and light. *quant-ph/0004053*, 2000.

[29] W. Wootters and W. Zurek. A single quantum cannot be cloned. *Nature*, 299:802–803, 1982.